SCIREA Journal of Physics
ISSN: 2706-8862
http://www.scirea.org/journal/Physics
January 15, 2023
Volume 8, Issue 1, February 2023
https://doi.org/10.54647/physics140515

A H atom model able to predict line series, fine structures, Fraunhofer and Fulcher spectra using a finite number of transversal electron orbits.

The atom radius size effect on hyperfine structure lines.

Emmanuel Saucedo-Flores, Víctor Manuel Rangel-Cobián

José Guadalupe Zuno No. 48, Industrial Los Belenes, CP 45101 Zapopan, Jalisco, México

Email: emmauel.saucedo@academicos.udg.mx; manuel.rangel@academicos.udg.mx

Abstract

A novel H atom model is devised using electron orbits located in planes not passing through the proton and are transversal or perpendicular to an axis originating at the proton center, and hence they are orthogonal to the longitudinal planes used in Bohr H atom model. The physical foundations for the proposed model are described and a straightforward expression for calculating the electron allowed energy levels is presented. A few calculation examples are provided and the obtained emission spectral lines are compared to the H spectral lines series, to the Fraunhofer absorption lines, to lines inside Fulcher bands and to the NREL AM0 irradiance spectrum. The transversal orbit model is shown to predict the appearance of the fine and

hyperfine electron emission structures. This is also the case if the atom radius, and consequently, the electron orbits are not considered rigid.

Keywords: Bohr model, emission line series, Rydberg energy, Fraunhofer spectrum, fine structure lines, Fulcher bands, NREL AM0 spectrum, the astronomical H lines, the non-rigid H atom.

Introduction

A brief summary of the H atom Bohr model [1] is given in the Appendix. Some shortcomings of the model are discussed in [2,3]. In the search of a possible fix, an alternative H model will be given here.

Foundation of the model

Let's start by developing an expression for the Rydberg energy or, equivalently, the H atom ionization energy, Ry (eV), in terms of the Coulomb force F_C (N) between the electron and the proton in the H atom. For this, the following physical interpretations of the Sommerfeld's or fine-structure constant, α, will be used

$$\alpha = \frac{v_1}{c} = \sqrt{\frac{2\text{Ry}}{E_e}} = \frac{1}{4\pi\varepsilon_0}\frac{e^2}{\hbar c} = k_e\frac{e^2}{\hbar c} = \frac{4\pi a_0}{\lambda_\infty} \tag{1}$$

where v_1 (m/s) is the electron orbital limit speed, c (m/s) is the speed of light in vacuum, a_0 (m) is the H Bohr radius, $E_e = m_e c^2$ (eV) is the electron energy-mass equivalent with m_e (kg) being the electron rest mass, e (C) is the electron charge, ε_0 (F/m) is the free space permittivity, k_e (N·m^2/C^2) is the Coulomb force constant, λ_∞ (m) is the Rydberg wavelength unit and $\hbar$ (J·s/cy) is the Planck constant divided by 2π. From (1), it follows that

$$\text{Ry} = \alpha^2\frac{E_e}{2e} = \left(\frac{v_1}{c}\right)^2\frac{E_e}{2e} = \frac{m_e v_1^2}{2e}\ \text{(eV)} \tag{2}$$

and also from (1)

$$\mathrm{Ry} = \alpha^2 \frac{E_e}{2} = \frac{v_1}{c}\frac{e^2}{4\pi\varepsilon_0\hbar c}\frac{m_e c^2}{2}\frac{a_0^2}{a_0^2} = \frac{e^2}{4\pi\varepsilon_0 a_0^2}\frac{a_0 v_1 m_e}{2\hbar}a_0 = \frac{a_0\alpha m_e c}{\hbar}\frac{a_0}{2e}\frac{e^2}{4\pi\varepsilon_0 a_0^2} = \frac{1}{e}\left[\frac{a_0}{2}F_C\right] \quad \text{(eV)} \tag{3}$$

where F_C (N) is the magnitude of the electrostatic centripetal force between the proton and the electron for a separation of a_0; above, the following expression in Classical Bohr radius [4] was used

$$a_0 = \frac{\hbar}{\alpha m_e c} = \frac{\hbar}{m_e v_1} \quad \text{(m)} \tag{4}$$

Then, merging (2) and (3), we obtain

$$\mathrm{Ry} = \frac{m_e v_1^2}{2e} = \frac{a_0 F_C}{2e} \quad \text{(eV).} \tag{5}$$

This implies that the Rydberg unit of energy is equal to the electron kinetic energy with an orbital escape speed of v_1 and, equivalently, to the electron moment of the Coulomb force with an arm length of only $a_0/2$.

Proposed model

Then, the possible electron orbits radii ought to be equal or shorter than $a_0/2$ which can be possible only if orbits are transversal, or orthogonal, to an axis along the proton center. This orbital concept is illustrated in Figure 1a) for the case of the electron longest possible orbit, or, atom ionization threshold. The Figure shows terms whose definitions are obtained by elaborating in (5) as follows

$$\mathrm{Ry} = \frac{m_e v_1^2}{2e} = 13.60569 \quad \text{(eV).} \tag{6}$$

and

$$\mathrm{Ry} = \frac{a_0 F_C}{\sqrt{2}\sqrt{2}e} = \frac{a_0 \sin(\beta_M) F_C \sin(\beta_M)}{e} = \frac{a_{0V} F_{CV}}{e} \quad \text{(eV).} \tag{7}$$

where $-F_{CV} = F_C \sin(\beta_M)$ (N) is the centripetal Coulomb force acting upon the electron and $a_{0V} = a_0 \sin(\beta_M)$ (m) is the electron orbit radius. $a_{0H} = a_0 \cos(\beta_M)$ (m) is the center point of the electron orbit and also represents the distance from the transversal orbital plane to the atom center. β_M represents the maximum cone angle established by the electron orbit, any other β-angle ought to be smaller. Figure 1*b*) depicts the a_{0V} and a_{0H} normalized functions for the β continuous case.

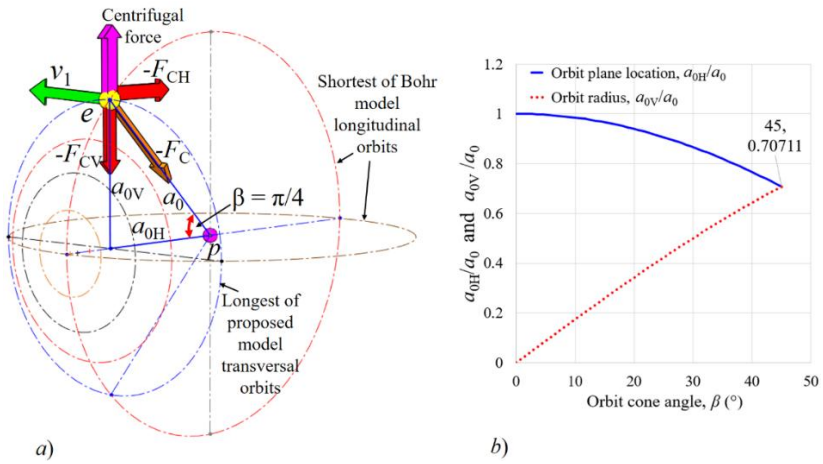

Figure 1. *a*) Schematics of the electron Coulomb forces and its speed for the longest of the proposed H transversal orbit model, that is, the brink of the atom ionization. *b*) β-dependence on the a_0-normalized distance of the orbit plane to the atom origin and the electron orbit radius.

Now, given that (6) and (7) on their left side have the maximum value of a quantized energy parameter and on its right side have constant valued parameters whose numerical value matches Ry; in (7) this happens owing to the help of the trigonometric terms which also ought to be quantized. This implies that the electrostatic force components and the transversal arm radial components are also quantized; the same can be said for the electron speed.

For the conditions described above, the Bohr model inverse squared dependence [1] on the quantum number n of the electron allowed energy levels E_n expression (e) in the Appendix would not be appropriate for the proposed model here. Instead, we'll suppose that the number of allowed energy levels is not infinite and establish a finite M number of transversal orbits and energy levels as follows

$$E_n = \mathrm{Ry}\left(\frac{n}{M}\right)^2 = \frac{m_e v_1^2}{2e}\left(\frac{n}{M}\right)^2 = \frac{a_0 F_C}{2e}\left(\frac{n}{M}\right)^2 = \frac{F_C}{2em_e v_1}\hbar\left(\frac{n}{M}\right)^2 \quad (\mathrm{eV}) \qquad n = 1,2,3,\ldots,M \tag{8}$$

where a_0 in (4) was used in last equality to remind the fundamental Bohr assumption on the electron angular momentum quantization is also present and write it as

$$L_n = 2e\frac{E_n}{F_C}m_e v_1 = \hbar\left(\frac{n}{M}\right)^2 \quad (\mathrm{J\cdot s}) \qquad n = 1,2,3,\ldots,M \tag{9}$$

see (a) in Appendix.

From (8) and (7), follows

$$r_n = a_{0V}\frac{n}{M} = a_0 \sin(\beta_M)\frac{n}{M} \text{ (m)},\ s_n = v_1\frac{n}{M} \text{ (m)},\ F_{CV,n} = F_{CV}\frac{n}{M} = F_C \sin(\beta_M)\frac{n}{M} \text{ (N)}, \quad n = 1,2,3,..,M \tag{10}$$

where r_n (m) is the n-orbit radius, s_n (m/s) is the corresponding electron speed, and $F_{CV,n}$ is the centripetal electrostatic force component acting on the electron along the n-orbit radius.

Using (10) in (9), it follows that, for any n quantum number, the electron centripetal and centrifugal forces are equal, that is

$$E_{c,n} = \frac{m_e s_n^2}{r_n} = F_{CV,n} \text{ (N)} \quad n = 1,2,3,...,M \tag{11}$$

where $E_{c,n}$ (N) is the electron centrifugal force for the n-orbit. For the sake of clarification clarification, F_C, defined in (3), does not change for this model because the electron to proton distance is always a_0. (11) is an equivalent expression to (b) in Appendix.

Emitted wavelengths

In order to calculate the emitted photon wavelengths for electron transitions from an $n = i > 1$ initial level to a final $n = f$ level with $f < i$, let's write the corresponding level energies as follows

$$E_i = Ry\left(\frac{i}{M}\right)^2 \text{ and } E_f = Ry\left(\frac{f}{M}\right)^2 \text{ (eV) for } i = 2,3,\ldots,M \text{ and } f < i \tag{12}$$

so that, the involved energy gap between the two levels is

$$E_{f,i} = E_i - E_f = \text{Ry}\frac{i^2 - f^2}{M^2} \text{ (eV) for } i = 2,3,\ldots,M \text{ and } f < i \tag{13}$$

Then, using the Einstein energy-wavelength equation in eV $\leftrightarrow$ nm units, it follows that the electron transition produces a photon wavelength of

$$\lambda_{f,i} = \frac{hc/e}{E_{f,i}}10^9 \approx \frac{1239.84}{Ry}\frac{M^2}{i^2 - f^2} = \lambda_\infty \frac{M^2}{i^2 - f^2}10^9 \approx 91.1267\frac{M^2}{i^2 - f^2} \text{ (nm) for } i = 2,3,\ldots,M \text{ and } f < i \tag{14}$$

where $\lambda_\infty = 9.11267951\text{x}10^{-8}$ (m).

Calculation examples

For a H system with M = 2, the possible energy levels are E_2 = 13.6022 and E_1 = 3.4014 eV, Figure 2 depicts the corresponding electron orbit location and force diagrams. This system will emit only one wavelength of magnitude of $\lambda_{2,1} = 121.53$ (nm) which is known as Lyman-α.

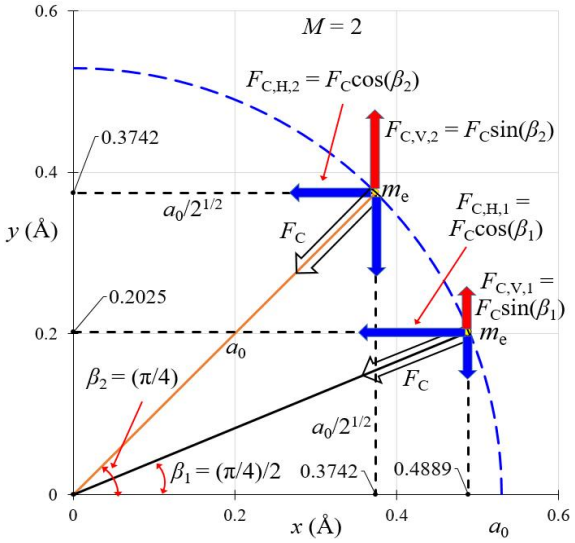

Figure 2. Electron force diagram for a 2-transversal orbit H model.

Orbit locations and corresponding energy levels for M = 4 and 24 are illustrated in Figure 3. Note that all labeled energy levels appear in Table I of the Appendix.

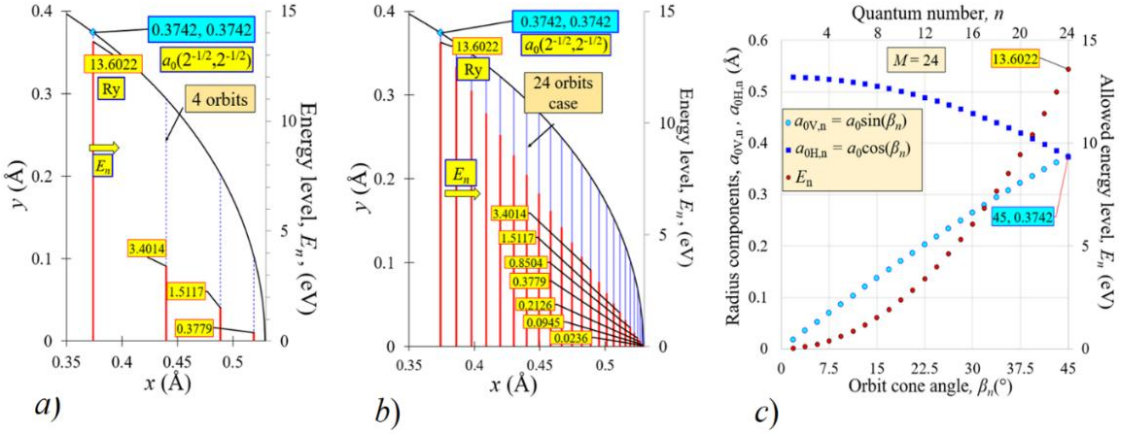

Figure 3. Transversal orbits and corresponding electron allowed energy levels for M = 4, *a*), and for M = 24, *b*). *c*) shows the orbit radius components and electron allowed energy levels for M = 24 as a function of the quantum number n and the orbit cone angle β_n.

Wavelength inventories for a few small *M* cases

To evaluate the capability of the proposed model on regards to matching the observed H wavelengths, five *M* values were considered, namely, 6, 10, 12, 14, and 15. Table A presents the five obtained wavelengths inventories. As can be observed, the *M* = 6, 12 cases provide wavelengths relating to five of the six H line series including 6 of their extreme values. An Ry value of 13.022 eV was used seeking to make the Balmer-α line equal to 656.28 nm, as in Fraunhofer C-line spectrum. The forthcoming calculation examples will all have a multiple of 6 *M* value.

Table A. Wavelengths inventories for *M* = 6, *a*), 10, *b*), 12, *c*), 14, *d*), and 15, *e*), transversal orbit models. Bold-typed data correspond to H line series extreme values.

Lyman Balmer Paschen Brackett Pfund Humphreys

M = 6 case. Wavelength λ_{if} (nm)

E_f (eV)		0.378	1.511	3.401	6.045	9.45
E_i (eV)	$i \setminus f$	1	2	3	4	5
13.6022	6	93.8	102.5	**121.5**	164.1	298.3
9.4460	5	136.7	156.3	205.1	**364.60**	
6.0454	4	218.8	273.5	468.8		
3.4006	3	410.2	**656.28**			
1.5114	2	1093.8				

a)

M = 10 case. Wavelength λ_{if} (nm)

E_f (eV)		0.136	0.544	1.224	2.176	3.40	4.897	6.67	8.71	11.02
E_i (eV)	$i \setminus f$	1	2	3	4	5	6	7	8	9
13.6022	10	92.1	94.9	100.2	108.5	**121.5**	142.4	178.7	253.2	479.7
11.0178	9	113.9	118.4	126.6	140.2	162.8	202.6	284.8	536.2	
8.7054	8	144.7	151.9	165.7	189.9	233.7	325.5	607.7		
6.6651	7	189.9	202.6	227.9	276.2	379.8	701.2			
4.8968	6	260.4	284.8	337.6	455.8	828.6				
3.4006	5	379.8	434.0	569.7	1012.8					
2.1764	4	607.7	759.6	1302.1						
1.2242	3	1139.4	1823.0							
0.5441	2	3038.3								

b)

M = 12 case. Wavelength λ_{if} (nm)

E_f (eV)		0.094	0.378	0.850	1.511	2.36	3.401	4.63	6.05	7.65	9.45	11.43
E_i (eV)	$i \setminus f$	1	2	3	4	5	6	7	8	9	10	11
13.6022	12	91.8	93.8	97.2	102.5	110.3	**121.5**	138.2	164.1	208.3	298.3	570.7
11.4296	11	109.4	112.2	117.2	125.0	136.7	154.4	182.3	230.3	328.1	625.0	
9.4460	10	132.6	136.7	144.2	156.3	175.0	205.1	257.4	**364.6**	690.8		
7.6512	9	164.1	170.5	182.3	201.9	234.4	291.7	410.2	772.1			
6.0454	8	208.3	218.8	238.6	273.5	336.6	468.8	875.0				
4.6285	7	273.5	291.7	328.1	397.7	546.9	1009.7					
3.4006	6	375.0	410.2	486.1	**656.28**	1193.2						
2.3615	5	546.9	625.0	**820.4**	**1458.4**							
1.5114	4	875.0	1093.8	**1875.1**								
0.8501	3	1640.7	2625.1									
0.3778	2	4375.2										

c)

M = 14 case. Wavelength λ_{if} (nm)

E_f (eV)		0.069	0.278	0.625	1.110	1.73	2.498	3.40	4.44	5.62	6.94	8.40	9.99	11.73
E_i (eV)	$i \setminus f$	1	2	3	4	5	6	7	8	9	10	11	12	13
13.6022	14	91.6	93.0	95.5	99.3	104.5	111.7	**121.5**	135.3	155.4	186.1	238.2	343.6	661.7
11.7284	13	106.3	108.3	111.7	116.8	124.1	134.3	148.9	170.1	203.0	258.9	372.2	714.6	
9.9935	12	124.9	127.6	132.3	139.6	150.1	165.4	188.1	223.3	283.6	406.0	776.8		
8.3973	11	148.9	152.7	159.5	170.1	186.1	210.2	248.1	313.4	446.6	850.7			
6.9399	10	180.5	186.1	196.3	212.7	238.2	279.1	350.3	496.3	940.3				
5.6213	9	223.3	232.0	248.1	274.9	319.0	397.0	558.3	1050.9					
4.4415	8	283.6	297.8	324.8	372.2	458.1	638.1	1191.0						
3.4006	7	372.2	397.0	446.6	541.4	744.4	1374.3							
2.4984	6	510.4	558.3	661.7	893.3	1624.1								
1.7350	5	744.4	850.7	1116.6	1985.0									
1.1104	4	1191.0	1488.8	2552.2										
0.6246	3	2233.2	3573.1											
0.2776	2	5955.1												

d)

M = 15 case. Wavelength λ_{if} (nm)

E_f (eV)		0.060	0.242	0.544	0.967	1.51	2.176	2.96	3.87	4.90	6.05	7.31	8.71	10.22	11.85
E_i (eV)	$i \setminus f$	1	2	3	4	5	6	7	8	9	10	11	12	13	14
13.6022	15	91.6	92.8	94.9	98.1	102.5	108.5	116.5	127.4	142.4	164.1	197.2	253.2	366.2	707.2
11.8490	14	105.2	106.8	109.7	113.9	119.9	128.2	139.5	155.4	178.3	213.6	273.5	394.4	759.6	
10.2168	13	122.1	124.3	128.2	134.0	142.4	154.2	170.9	195.3	233.1	297.2	427.3	**820.4**		
8.7054	12	143.4	146.5	151.9	160.2	172.3	189.9	215.9	256.4	325.5	466.1	891.7			
7.3150	11	170.9	175.3	183.1	195.3	213.6	241.3	284.8	359.8	512.7	976.6				
6.0454	10	207.2	213.6	225.4	244.2	273.5	320.4	402.1	569.7	1079.4					
4.8968	9	256.4	266.3	284.8	315.5	366.2	455.8	640.9	1206.4						
3.8691	8	325.5	341.8	372.9	427.3	525.9	732.5	1367.3							
2.9623	7	427.3	455.8	512.7	621.5	854.5	1577.6								
2.1764	6	586.0	640.9	759.6	1025.4	1864.4									
1.5114	5	854.5	976.6	1281.8	**2278.8**										
0.9673	4	1367.3	1709.1	2929.8											
0.5441	3	2563.6	4101.8												
0.2418	2	6836.3													

e)

M = 48 case

a) Comparison with H line series, Fraunhofer spectrum and Fulcher bands.

The electron allowed energy levels for a maximum transversal orbit number of *M* = 48 are plotted in Figure 4 *a*) and compared against the first 48 energy levels for the H Bohr model. Note the big difference in energy span for reaching the first 24 energy levels for each model. For the Bohr model the energy delta is E_{24} - E_1 = - 0.024 - (-13.602) = 13.58 eV - very near to the ionization energy level - while for the transversal orbit model the energy shift is E_{24} - E_1 = 3.401 - 0.0059 = 3.395 eV only.

Figure 4. *b*) gives a comparison of how the quantum number impacts the electron orbit radius for the Bohr H atom model and the electron transversal radius for the $M = 48$ model case. For $n = 1$ to 48, the Bohr model calls for a radius increase of 2304 times and the electron energy is short to the ionization level by 0.0059 eV; for the proposed model, the increment of the electron transversal radius case is of only 43.22 times for $m = 1$ to M and the electron energy is Ry.

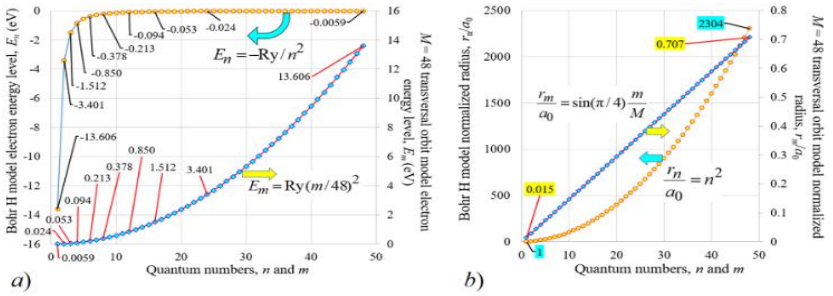

Figure 4. *a*) Comparison of the allowed electron energy levels for the Bohr H atom model up to $n = 48$ and all the energy levels in the proposed transversal orbit model for $M = 48$. *b*) Corresponding electron normalized orbit radius for each quantum number and model case.

Figure 5.*a* portrays the Bohr model emitted photon wavelengths for electron transitions into end quantum levels $f = 1, 2, 3, 4, 5$ and 6 which correspond to Lyman, Balmer, Paschen, Brackett, Pfund and Humphreys line series, respectively. Note that for each line series there is a continuum wavelength range whose experimental evidence has not yet been provided. Figure 5.*b* plots the emitted photon wavelengths involving only electron transitions between even quantum numbers for the transversal orbit model with $M = 48$ to which was added a near zero level to obtain 5 wavelength

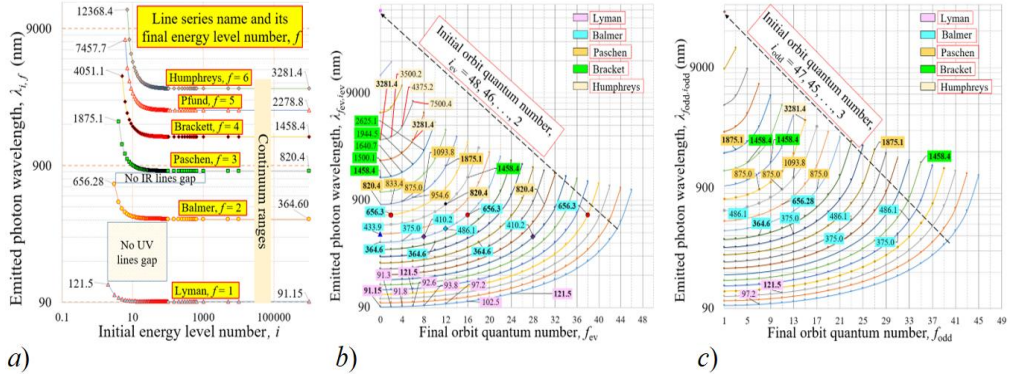

Figure 5. *a*) Plot of emitted photon wavelengths in common line series of Bohr H atom model. Photon wavelengths involving electron transitions only between even quantum numbers for the proposed model with $M = 48$; a near zero (2.3E-5 eV) level was added for the sake of comparison with line series extreme values in Figure 4 *b*). *b*) Photon wavelengths involving electron transitions only between odd quantum numbers.

(short) limits appearing in above mentioned H line series; note that 4 of these wavelength limits show at least a two-fold multiplicity without involving the added near zero level. Figure 5.*c* depicts the emitted photon wavelengths involving only odd to odd quantum numbers electron transitions. It's worth mentioning that none of the Pfund line series limits appear for this *M* value; the only three Pfund series wavelengths values are not indicated in Figure 5. Other *M* values for this model, for example multiples of 15 or 20, provide both Pfund line series limits and several other of its lines.

Table B gives the inventory of emitted photon wavelengths for electron transitions with an even initial quantum number for the $M = 48$ transversal orbit model case. Similarly, Table C provides all the wavelengths for electron transitions starting in an odd quantum number. Without considering transitions into the "zero" energy level, the $M = 48$ transversal orbit model case gives rise to only 1128 allowed electron transitions (47*24); while for $M = 96$ the electron transitions amount to 4656.

Table B. *M* = 48 transversal orbit model inventory of wavelengths for electron transitions involving an even initial quantum number. Data in f_{ev} = "0" eV row don't correspond to the model and are just for the sake of reference.

	Lyman		Balmer			Paschen			Brackett			Pfund			Humphreys			> 6 order series				Fraunhofer			Fulcher	
$E_{i,ev}$ eV	0.024	0.094	0.213	0.378	0.590	0.850	1.157	1.511	1.913	2.361	2.857	3.401	3.99	4.63	5.31	6.05	6.82	7.65	8.52	9.45	10.41	11.43	12.49	**13.6022**		
Photon wavelengths for transitions from even initial state to even final state quantum numbers $i_{ev} \rightarrow f_{ev}$																										$E_{f,ev}$
	2	4	6	8	10	12	14	16	18	20	22	24	26	28	30	32	34	36	38	40	42	44	46	48		eV
$E_{f,odd}$	52554	13129	**5834**	**3281.6**	2100	**1458.4**	1072	**820.4**	648.2	525.0	433.9	**364.6**	311	268	233	205.1	181.7	162.0	145.4	131.3	119.1	108.5	99.2	**91.15**	"0"	2.3E-05
eV		17501	6563	3500	2188	1500.1	1094	833.4	**656.28**	530	437.5	367.2	313	269.2	234.4	205.9	182.3	162.5	145.8	131.6	119.3	108.7	99.4	91.31	2	0.024
13.041	47 2211		10500	4375	2500	1640.7	1167	875.0	682	546.9	449	375.0	318	273.5	237.6	208.3	184.2	164.1	147.1	132.6	120.1	109.4	100.0	91.79	4	0.094
11.955	45 753	2307.8		7500	**3281.4**	1944.5	1313	954.6	729	577.0	468.8	388.9	328	280.8	243.1	212.6	187.5	166.7	149.2	134.3	**121.53**	110.5	101.0	92.60	6	0.213
10.916	43 462	787	2414		**5833.6**	2625.1	1591	1093.8	808	625	500	410.2	343	291.7	251.2	218.8	192.3	170.5	152.2	136.7	123.5	112.2	102.3	93.75	8	0.378
9.924	41 337.1	482.8	823.6	2530		4773	2188	1346.2	938	700	546.9	441	**364.6**	307	262.5	227.3	198.9	175.6	156.3	140.0	126.2	114.4	104.2	95.3	10	0.590
8.980	39 268.2	353	506.0	864	2658		4039	**1875.1**	1167	**820.4**	618	486.1	394.8	328	277.8	238.6	207.5	182.3	161.5	144.2	129.6	117.2	106.5	97.2	12	0.850
8.082	37 224.6	281.1	370	532	909	2800		3500	1640.7	1029	729	553	437.5	357.2	298.3	253.6	218.8	190.9	168.3	149.6	133.9	120.7	109.4	99.6	14	1.157
7.232	35 194.6	235.7	295.4	390	560	959	2958		3088	**1458.4**	921	**656.28**	500	397.7	326	273.5	233.3	201.9	176.8	156.3	139.3	125.0	112.9	102.5	16	1.511
6.429	33 172.8	204.5	247.9	311	411	592	1015	3134		2763.3	1313	833.4	597	457	**364.6**	300.0	252.4	216.1	187.5	164.6	145.8	130.3	117.2	106.1	18	1.913
5.673	31 156.4	181.8	215.4	261.5	329	434.8	626.9	1077	3333		2500	1193.2	760.9	546.9	420	337	277.8	234.4	201.2	175.0	154.0	136.7	122.4	110.3	20	2.361
4.965	29 143.5	164.7	191.8	227.5	276.7	348	462	666.7	1148	3559		2282.7	1094	700	504.8	388.9	313	258.6	218.8	188.2	164.1	144.6	128.7	115.4	22	2.857
4.304	27 133.3	151.4	174.0	202.9	241.1	293.7	370	492	712	1228	3818		2100	1010	648.2	468.8	362	291.7	241.9	205.1	176.8	154.4	136.4	**121.53**	24	3.401
3.690	25 125.1	140.9	160.2	184.4	215.4	256.4	313	395.5	526.3	764	1321	4118		1945	938	603	437.5	339	273.5	227.3	193.0	166.7	145.8	129.0	26	3.991
3.123	23 118.3	132.3	149.3	170.0	196.1	229.5	273.8	335	424	566	823.6	1429	4468		1810	875.0	565	410.2	318	257.4	214.3	182.3	157.7	138.2	28	4.629
2.604	21 112.7	125.4	140.5	158.7	181.2	209.4	245.6	293.7	360	458	612	894	1556	4884		1694	**820.4**	530	386	300.0	243.1	202.7	172.7	149.6	30	5.313
2.131	19 108.1	119.7	133.3	149.7	169.5	193.9	224.6	264.2	317	390	496.5	666.7	977	1707	5385		1591	772	500	**364.6**	283.8	230.3	192.3	164.1	32	6.045
1.706	17 104.2	114.9	127.5	142.4	160.2	181.8	208.5	242.2	285.7	344	424	543	732	1077	1892	6000		1500	729	473	345	269.2	218.8	182.9	34	6.82
1.328	15 101.0	111.1	122.7	136.5	152.7	172.3	196.1	225.6	262.8	311	376	465.7	598	811	1200	2121	6775		1419	690.8	449	328	256.1	208.3	36	7.65
0.998	13 98.4	107.9	118.9	131.7	146.8	164.7	186.3	212.8	245.6	287.3	341	414	516.0	666.7	909	1355	2414	7778		1346	**656.28**	427	313	244.2	38	8.52
0.714	11 96.2	105.3	115.7	127.8	142.0	158.7	178.7	202.9	232.6	269.6	317	378	462	578.5	753	1035	1556	2800	9131		1280.5	625	407	298.3	40	9.45
0.478	9 94.5	103.2	113.2	124.8	138.3	154.1	172.8	195.4	222.7	256.4	298.7	353	424	521	658	864	1200	1826	3333	11053		1221	597	388.9	42	10.41
0.289	7 93.1	101.6	111.3	122.5	135.4	150.5	168.4	189.7	215.4	246.8	285.7	335	398.5	483	598	764	1015	1429	2211	4118	14001		1167	571	44	11.43
0.148	5 92.1	100.4	109.9	120.8	133.3	148.0	165.2	185.7	210.2	240.0	276.7	323	381	458	560	702	909	1228	1765	2800	5385	19092		1117.1	46	12.49
0.053	3 91.5	99.7	109.0	119.7	132.0	146.3	163.2	183.1	206.9	235.7	271.0	315	370	442	537.1	666.7	850	1123	1556	2308	3818	7778	30001			
0.006	1 91.19	99.3	108.5	119.1	131.3	145.5	162.2	181.8	205.3	233.6	268.2	311	365.2	434.8	526.3	650	823.6	1077	1469	2121	3333	6000	14001	70003		
	48	46	44	42	40	38	36	34	32	30	28	26	24	22	20	18	16	14	12	10	8	6	4	2		
Photon wavelengths for transitions from even initial state to odd final state quantum numbers $i_{ev} \rightarrow f_{odd}$																										
$E_{i,ev}$ eV	**13.6022**	12.49	11.43	10.41	9.446	8.525	7.651	6.825	6.045	5.313	4.629	3.991	3.401	2.857	2.361	1.913	1.511	1.157	0.850	0.590	0.378	0.213	0.094	0.024		

Odd final state quantum numbers f_{odd}

Even final state quantum numbers f_{ev}

Table C. M = 48 transversal orbit model inventory of wavelengths for electron transitions involving an odd initial quantum number.

	Lyman		Balmer			Paschen			Brackett			Pfund			Humphreys			> 6 order series			Fraunhofer			Fulcher		
$E_{i,odd}$ eV		0.053	0.148	0.289	0.478	0.714	0.998	1.328	1.706	2.131	2.604	3.123	3.690	4.304	4.965	5.673	6.429	7.232	8.082	8.980	9.92	10.92	11.96	13.041		
Photon wavelengths for level transitions from odd initial state to even final state quantum numbers $i_{odd} \rightarrow f_{ev}$																										$E_{f,ev}$
$E_{f,odd}$		3	5	7	9	11	13	15	17	19	21	23	25	27	29	31	33	35	37	39	41	43	45	47			eV
eV		42002	10000	4667	2727	1795	1273	950	737	588.3	480.6	400	338.2	289.7	250.9	219.4	193.6	172.0	153.9	138.4	125.2	113.8	103.9	95.2	2		0.024
11.955	45 1141		23334	6364	3231	2000	1373	1005	769	609	494	409	344.8	294.5	254.6	222.2	195.7	173.7	155.2	139.5	126.1	114.6	104.5	95.8	4		0.094
10.916	43 583	1193		16155	4667	2471	1579	1111	830	646.2	518.5	426.0	356.6	303.0	260.9	227.0	199.4	176.6	157.5	141.4	127.7	115.8	105.6	96.6	6		0.213
9.924	41 397.7	610	1250		12354	3684	2000	1304	933	707.1	557.1	452	374.3	316	270.3	234.1	204.9	180.9	160.9	144.1	129.9	117.7	107.1	97.9	8		0.378
8.980	39 305	417	640	1313		10000	3044	1680	1111	805	616	489.5	400	334	283.4	243.9	212.3	186.7	165.5	147.8	132.8	120.1	109.1	99.6	10		0.590
8.082	37 250.0	320	437.5	673	1382		8400	2593	1448	967.8	707	545.5	436.6	359.0	301.3	257.0	222.2	194.3	171.4	152.5	136.6	123.2	111.6	101.7	12		0.850
7.232	35 213.4	262.5	336.6	461	709	**1458.4**		7242	2258	1273	857	631	490	394	325.6	274.5	235.2	204.1	179.0	158.5	141.4	127.0	114.8	104.3	14		1.157
6.429	33 187.5	224.4	276.3	354.7	486.1	750	1544		6364	2000	1135	769	569	444	359.0	297.9	252.1	216.7	188.7	166.0	147.4	131.8	118.7	107.5	16		1.511
5.673	31 168.3	197.4	236.5	291.7	375.0	514.7	795	1641		5676	1795	1024	698	518.5	406.2	330	274.5	233.1	201.0	175.4	154.8	137.7	123.5	111.4	18		1.913
4.965	29 153.5	177.4	208.3	250.0	309	397.7	547	846.8	1750		5122	1628	933	638	476.2	374.3	304.8	254.6	216.7	187.3	163.9	144.9	129.2	116.1	20		2.361
4.304	27 141.9	162.0	187.5	220.6	265.2	328	423.4	583	905	**1875.1**		4667	1489	857	588.3	440.3	347.1	283.4	237.3	202.5	175.4	153.9	136.3	121.7	22		2.857
3.690	25 132.6	150.0	171.6	198.9	234.4	282.3	350	453	625	972	2019		4286	1373	792	545.5	409.4	323.6	264.8	222.2	190.1	165.0	144.9	128.6	24		3.401
3.123	23 125.0	140.4	159.1	182.3	211.7	250.0	301.7	375.0	486.1	673	1050	2188		3962	1273	737	508.5	382.5	303.0	248.5	209.0	179.0	155.7	137.0	26		3.991
2.604	21 118.8	132.6	149.2	169.4	194.5	226.3	267.9	324	404	525.0	729	1141	2386		3684	1186	688.6	476.2	359.0	285.0	234.1	197.2	169.2	147.4	28		4.629
2.131	19 113.6	126.2	141.1	159.1	181.0	208.3	243.1	288.5	350	437.5	571	795	1250	2625.1		3443	1111	646.2	448	338.2	268.9	221.3	186.7	160.4	30		5.313
1.706	17 109.4	121.0	134.6	150.9	170.5	194.5	224.4	262.5	313	380.5	477.3	625	875.0	1382	2917		3231	1045	609	422.6	320	254.6	209.8	177.2	32		6.045
1.328	15 105.9	116.7	129.3	144.2	162.0	183.6	210.0	243.1	285.3	341	417	525.0	691	972	1544	**3281.4**		3044	986.0	575	400	303.0	241.7	199.4	34		6.825
0.998	13 102.9	113.2	125.0	138.9	155.3	175.0	198.9	228.3	265.2	313	375.0	461	583	772	1093.8	1750	3750.2		2877	933	545.5	380	288.1	230.0	36		7.651
0.714	11 100.6	110.3	**121.53**	134.6	150.0	168.3	190.2	217.0	250.0	291.7	345	417	514.7	**656.28**	875.0	1250	2019	4375		2727	886.1	518.5	361	274.5	38		8.525
0.478	9 98.7	108.0	118.8	131.3	145.8	163.1	183.6	208.3	238.6	276.3	324	386	468.8	583	750	1010	**1458.4**	2386	5250		2593	843.4	494.1	344.8	40		9.446
0.289	7 97.2	106.3	116.7	128.7	142.7	159.1	178.6	201.9	230.3	265.2	309	**364.6**	437.5	535.7	673	875.0	1193	1750	2917	6563		2470.7	805	471.9	42		10.414
0.148	5 96.2	105.0	115.1	126.8	140.4	156.3	175.0	197.4	224.4	257.4	298.3	350	417	504.8	625	795	1050	**1458.4**	2188	3750	8750		2359.7	769	44		11.430
0.053	3 95.5	104.2	114.1	125.6	138.9	154.4	172.7	194.5	220.6	252.4	291.7	341	404	486.1	597	750	972	1313	**1875.1**	2917	5250	13126		2258.2	46		12.492
0.0059	1 95.1	103.8	113.6	125.0	138.2	153.5	171.6	193.0	218.8	250.0	288.5	336.6	397.7	477.3	583	729	938	1250	1750	2625	4375	8750	26251				
	47	45	43	41	39	37	35	33	31	29	27	25	23	21	19	17	15	13	11	9	7	5	3	1			
Photon wavelengths for level transitions from odd initial state to odd final state quantum numbers $i_{odd} \rightarrow f_{odd}$																										
$E_{f,odd}$ eV	13.041	11.96	10.92	9.924	8.980	8.082	7.232	6.429	5.673	4.965	4.304	3.690	3.123	2.604	2.131	1.706	1.328	0.998	0.714	0.478	0.289	0.148	0.053	0.006		

Odd final state quantum numbers f_{odd} — Even final state quantum numbers f_{ev}

In Table B, the zigzagged red lines demark transitions with either a maximum initial quantum number of 24 (3.4 eV highest electron excitation energy) or a number of energy levels among the transitions equal or lower than 6. In Figure Table C, the red lines demark transitions with either a maximum initial quantum number of 23 or to a number levels among the transitions equal or lower than 6.

It is worth noting that even to even (top to right) transitions in top triangle of Table B and odd to odd (bottom to left) transitions in bottom triangle of Table C have numerous bold data which identify H line series limits, mostly appearing inside the red line demarcation; on the contrary, none of these wavelengths appear on the opposite triangles of both tables where $even \Leftrightarrow odd$ quantum numbers transitions are involved. Three notorious cases are the four-fold multiplicity observed for the Balmer series lines known as $H\alpha$ = 656.28 nm and $H\beta$ = 486.1 nm and also the five-fold multiplicity for the shortest wavelength of the Bracket line series 1458.4 nm.

Data in yellow-colored cells in Tables B and C correspond, within ± 1.5 nm, to absorption lines in Fraunhofer spectrum [5,6] while data in tortilla-colored cells are lines appearing in emitting Fulcher bands [7,8,9,10,11], see Figure 6. There are a few other Fulcher band under 400 nm

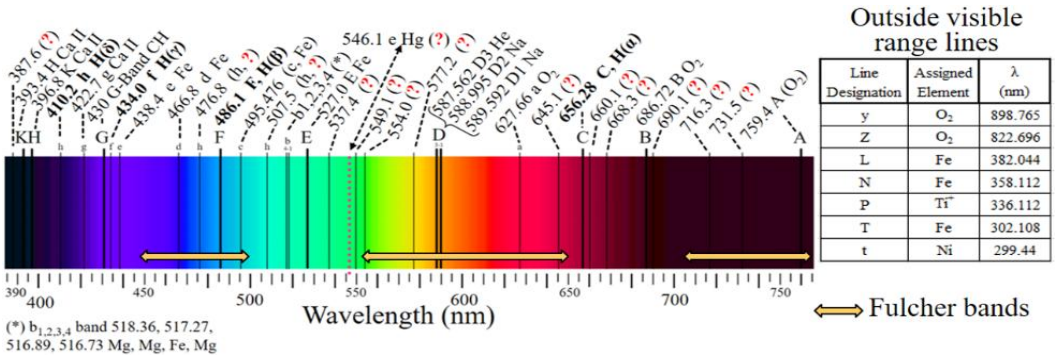

Figure 6. Fraunhofer solar visible spectral lines from data in and approximate location and extension of ranges of H emission Fulcher bands. Symbol (?) means none or partial line identification; the added 546.073 nm line with e-designation and assigned to Hg is tabulated but was missing in the spectrum.

From Tables B and C, it is possible to establish viable electron photon emitting transition sequences starting from any excitation energy level. Figure 7 portrays a partial inventory of such sequences for the Bohr model, *a*), and for the transversal orbit model with M = 48 levels, *b*) and *c*); for this case, the transition type involved is indicated at the top. It is patent the preponderance of the Fulcher bands electron transitions obtained with the transversal orbit model and the scarcity of them for the Bohr model.

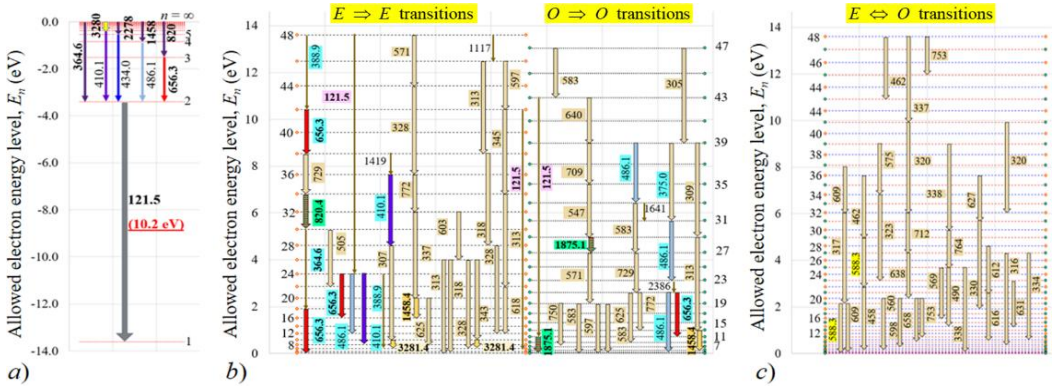

Figure 7. Electron emitting transition sequences for the H Bohr model, *a*), and for the transversal orbit model, *b*) and *c*).

Another outstanding difference among the two models is related to the number of possible transitions for a given excitation energy. In Bohr's model, for an exciting energy of about 12.1 eV the electron will reach just up to level n = 3 and will be able to undergo only 3 different emitting level transitions. For the transversal orbit model, the same exciting energy would make

the electron to reach the $n = 45$ energy level so that the possible emitting level transitions amount to 990.

b) Comparison with NREL AM0 solar spectrum.

Figures 8 to 10 provide a three segment comparison of the full presence inventory of the obtained wavelengths with the H transversal orbit model involving $M = 48$ energy levels with respect to the NREL AM0 solar irradiance [12]. H line series, Fraunhofer absorption line designations, and Fulcher band lines are highlighted with the same background color code as above.

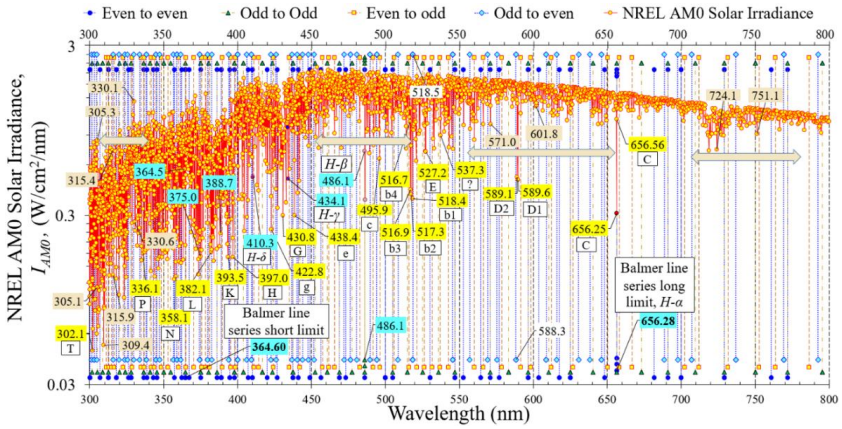

Figure 8. $M = 48$ transversal orbit model emitted photon wavelength line presence for all four electron transition types compared to the near UV-near IR range of the NREAL AM0 solar irradiance. H Balmer line series, Fraunhofer absorption lines, see Fig. 6, and locations of Fulcher main bands are highlighted.

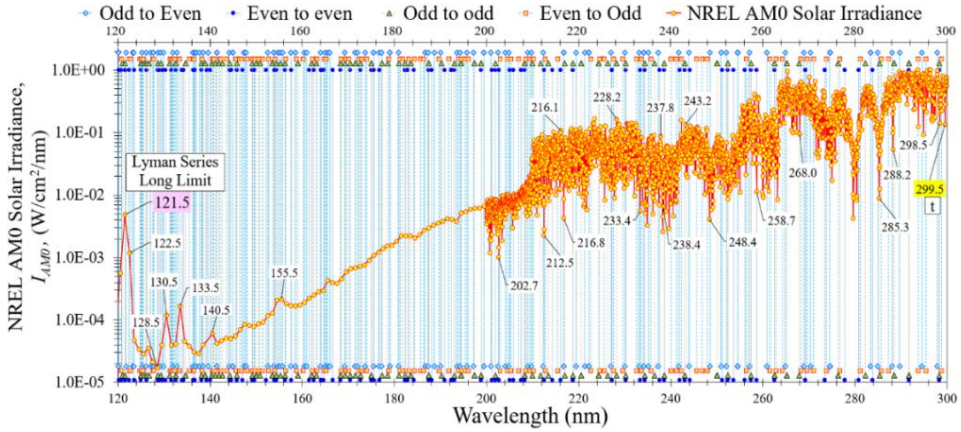

Figure 9. $M = 48$ transversal orbit model emitted photon wavelength line presence for all four electron transition types compared to UV data from two merged NREL AM0 solar irradiance spectra [3]; for wavelengths under 200 nm, the data step is 1.0 nm, above 200 nm, the data step is in the range of 0.024-0.054 nm. Of the Bohr H model, only the long limit of the Lyman spectral series appears on this wavelength range. Also, the shortest Fraunhofer absorption line is indicated.

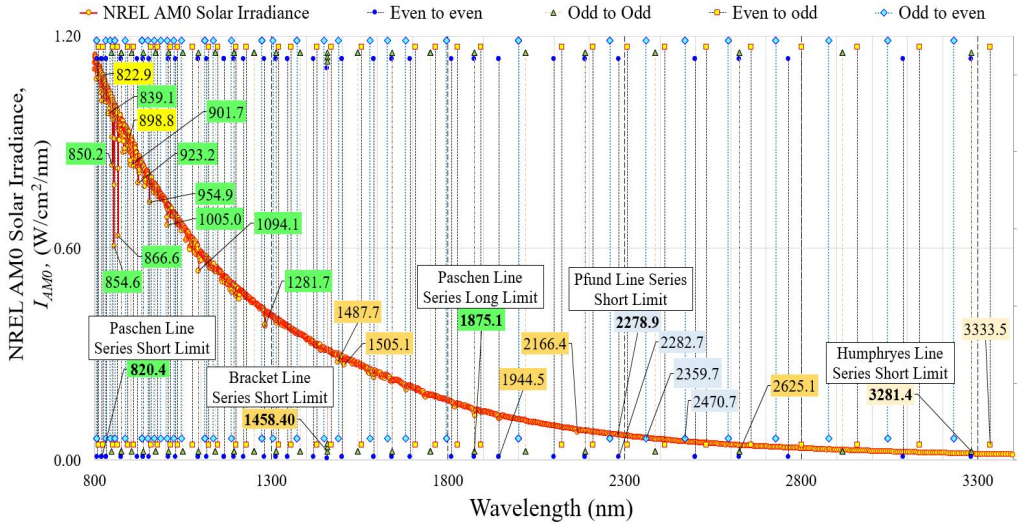

Figure 10. ***M*** **= 48 transversal orbit model wavelengths line presence for the 800-3400 nm range compared to the NREL AM0 solar spectral irradiance, I_{AM0}, H line series, and the two longest Fraunhofer lines.**

M = 144 and *M* = 216 level systems with fine structure line cases

From Table C and Figs. 6 and 8, it can be observed that the Fraunhofer three D lines and four b lines are poorly matched by the M = 48 model case; the nearest b1 wavelength is 518. 54 nm obtained with transitions $\lambda_{21,6} = \lambda_{27,18} = \lambda_{43,38}$; while inside the D band appears only the line of 588.26 nm for transitions $\lambda_{19,2} = \lambda_{29,22}$. An improved match to these bands can be obtained for systems with higher M values. This is exemplified for the cases M = 144 and M = 216 in Table D.

Table D. Fine structure lines on Fraunhofer lines D1, D2, D3 and $b_{1,2,3,4}$ for transversal orbit systems for *M* = 144, *a*), and for *M* = 216, *b*).

D1, D2, D3 band				$b_{1,2,3,4}$ band			
i	f	λ_{if} (nm)	E_{if} (eV)	i	f	λ_{if} (nm)	E_{if} (eV)
62	25	587.17	2.1116	76	46	516.42	2.4009
70	41			61	8	516.84	2.3989
79	55	587.71	2.1096	91	68		
140	128			116	99	517.12	2.3976
103	86	588.26	2.1076	64	21		
57	6			94	72	517.55	2.3956
73	46			65	24	517.97	2.3936
87	66			62	14	518.12	2.3930
84	62	588.45	2.1070	67	29		
130	117	588.63	2.1063	88	64		
94	75			73	41		
98	80	589.92	2.1017	129	114	518.54	2.3910
				63	18		
				81	54		

a)

D1, D2, D3 band								$b_{1,2,3,4}$ band							
i	f	λ_{if}(nm)	E_{if}(eV)	i	f	λ_{if}(nm)	E_{if}(eV)	i	f	λ_{if}(nm)	E_{if}(eV)	i	f	λ_{if}(nm)	E_{if}(eV)
191	171	587.389	2.1108	132	101	588.772	2.1058	100	42	516.355	2.4011	117	74	517.801	2.3944
200	181	587.471	2.1105	85	2	588.935	2.1052	114	69	516.418	2.4009	106	55	517.927	2.3939
92	35			139	110			98	37			190	167		
94	40	587.714	2.1096	114	76	589.017	2.1049	166	139			206	185		
210	192			85	3	589.343	2.1038	119	77	516.606	2.4000	94	25	518.116	2.3930
129	97	588.039	2.1084	104	60			91	7			93	21		
152	126	588.365	2.1073	175	153			125	86	516.794	2.3991	103	49		
126	93	588.446	2.1070	116	79	589.425	2.1035	198	176	516.857	2.3988	132	96		
86	13			88	23			138	104			92	16		
157	132	588.609	2.1064	112	73			111	64	517.046	2.3979	127	89		
85	1	588.690	2.1061	85	4	589.915	2.1017	135	100			183	159		
143	115			147	120			177	152			156	127	518.180	2.3927
107	65			123	89	589.997	2.1014	152	122	517.360	2.3965	99	40	518.559	2.3909
								91	8	517.549	2.3956	91	9	518.622	2.3906
								141	108			107	57		
								105	53	517.612	2.3953	215	195		
								171	145						
								148	117	517.675	2.3950				
								104	51						

b)

Table E provides, for the same set of M values, the Lyman series α-line and closer lines; the involved energy change in all transitions, E_{if} (eV), is also shown and has a mean energy step of ≈

0.9 meV which compares well to the level of the relativistic correction for the ground level given in [13,14].

Table E. *a*) gives the three-fold Lyman series α-line data for the $M = 48$ case discussed above and some close lines. Much closer lines to the Lyman series α-line appear for transversal orbit systems with $M = 144$, *b*), and with $M = 216$, *c*).

Lyman-α			
i	f	λ_{if} (nm)	E_{if} (eV)
42	5	120.76	10.2666
45	17	120.97	10.2489
42	6	121.53	10.2017
43	11		
48	24		
47	22	121.74	10.1839

a)

Lyman-α			
i	f	λ_{if} (nm)	E_{if} (eV)
134	49	121.51	10.2036
126	18	121.53	10.2017
127	24		
129	33		
144	72		
143	70	121.56	10.1997
125	9	121.60	10.1964
128	29		

b)

Lyman-α			
i	f	λ_{if} (nm)	E_{if} (eV)
195	55	121.51	10.2040
216	108	121.53	10.2017
189	27		
215	106	121.54	10.2008
188	19	121.56	10.1990
208	91		
214	104	121.58	10.1982
198	65		
199	68	121.59	10.1973
205	84	121.61	10.1949
187	1	121.62	10.1947
203	79		

c)

For the $M = 144$ and $M = 216$ cases, Table F portrays the fine structure lines corresponding to the Fraunhofer C-line or Balmer series α-line [14] along with the corresponding energy change among the involved transition levels.

Table F. *a*) Gives the ten-fold Balmer Hα-line data for the $M = 144$ case showing also three close lines. *b*) Three two-fold lines appear close to a nine-fold Hα-line for the transversal orbit systems with $M = 216$.

C-line (Balmer Hα)			
i	f	λ_{if} (nm)	E_{if} (eV)
55	12	656.053	1.88985
54	6	**656.281**	1.88919
56	16		
58	**22**		
61	29		
63	33		
72	48		
82	**62**		
89	71		
98	**82**		
126	114		
62	31	655.598	1.89116
79	**58**	656.965	1.88723

a)

C-line (Balmer Hα)			
i	f	λ_{if} (nm)	E_{if} (eV)
83	20	655.371	1.89182
165	144		
81	9	**656.281**	1.88919
84	24		
87	33		
101	61		
108	72		
123	93		
147	**123**		
172	152		
189	171		
180	161	656.382	1.88890
120	**89**		
89	38	656.585	1.88832
199	182		
142	117	656.788	1.88774
110	75		
106	69		

b)

The hyperfine structure line cases. The H galactic spectral lines.

The existence of a H astronomical line of 21 cm wavelength was first theoretically figured out by the Dutch astronomer H.C. Van de Hulst in 1945 [15] based on calculating the electron spin energy change when flipping its rotation orientation with respect to the proton rotation. For this to happen, the electron must be in its ground orbit energy level; then, it has to receive somehow enough magnetic energy to toggle its spin state from the lower energy anti-parallel rotation into the higher energy parallel rotation, which is about 5.8 μeV; finally, the electron has to swap back to its original spin state by releasing the excess energy via the emission of a photon whose wavelength is approximately 21.1 cm. This prediction was experimentally confirmed in 1951 by Ewen and Purcell [16] and by C.A. Muller and J.H. Oort, [17]

It turns out that the transversal orbit model with a high enough number of states; for example, an M = 2636 system predicts the presence of the 21.1 cm line for an electron transition among the two lowest energy states, see Table G. *a*); for M = 7908, this line appears in two transitions along with two other lines in the cm range; all of them involve electron allowed energy levels of less than 100 μeV; the accompanying transversal orbit radii are about 10^{-3} to 10^{-4} lower than a_0. Table G shows the calculated data for these two cases and are compared to the H Bohr model equivalent wavelengths. All the energy levels involved for these transitions are near the ionization energy of the atom and the corresponding electron orbit radii are about 10^4 to 10^5 higher than a_0.

Table G. *a*) 21.1 cm line earliest detection for the transversal obit model is obtained with M = 2636. *b*) M = 7908 provides two 21.1 cm lines along with the 28.3 cm and the 2.8 cm lines. *c*) the H Bohr model prediction of these lines. An Ry value of 13.60569 eV, (6), was used for these calculations.

n_i, n_f	Energy level, E_n (eV)	Energy gap, $E_{i,f}$ (μeV)	Wavelength, $\lambda_{i,f}$ (cm)
2	7.8323E-06	5.87	21.106
1	1.9581E-06		

a)

n_i, n_f	Energy level, E_n (eV)	Energy gap, $E_{i,f}$ (μeV)	Wavelength, $\lambda_{i,f}$ (cm)
18	7.0491E-05	44.17	2.807
11	2.6325E-05		
14	4.2643E-05	5.87	21.106
13	3.6768E-05		
6	7.8323E-06	5.87	21.106
3	1.9581E-06		
6	7.8323E-06	4.35	28.494
4	3.4810E-06		

b)

n_f, n_i	Energy level, E_n (eV)	Energy gap, $E_{i,f}$ (μeV)	Wavelength, $\lambda_{i,f}$ (cm)
106	-1.2109E-03	44.43	2.790
108	-1.1665E-03		
209	-3.1148E-04	5.88	21.097
211	-3.0560E-04		
231	-2.5497E-04	4.36	28.447
233	-2.5062E-04		
364	-1.0269E-04	4.37	28.377
372	-9.8318E-05		

c)

The radius size effect on the fine and hyperfine structure lines.

An alternative approach to derive the H astronomical lines can be devised by supposing that the H atom radius is not rigid and can be contracted or expanded upon an external stress. Then, using (5), (3) and (1) and elaborate as follows

$$\mathrm{Ry}=\frac{a_0 F_C}{2e}=\frac{a_0}{2e}\frac{e^2}{4\pi\varepsilon_0 a_0^2}=\frac{ek_e}{2}\frac{1}{a_0}\Rightarrow\frac{ek_e}{2}=a_0\mathrm{Ry}\quad(\mathrm{eV}) \tag{15}$$

Differentiating (15) provides

$$\Delta\mathrm{Ry}=\frac{ek_e}{2}\Delta\{\frac{1}{a_0}\}=-\frac{ek_e}{2}\frac{\Delta a_0}{a_0^2}=-\mathrm{Ry}\frac{\Delta a_0}{a_0}=-\mathrm{Ry}\frac{a_{0,new}-a_0}{a_0}\quad(\mathrm{eV}) \tag{16}$$

where $a_{0,new}$ is a higher or lower value of the H atom radius produced as a result of an energy exchange with its surroundings. Let's define a new Rydberg energy as Ry_{new} so (16) becomes

$$\mathrm{Ry}_{new}=\mathrm{Ry}+\Delta\mathrm{Ry}=\mathrm{Ry}(1+\frac{a_0-a_{0,new}}{a_0})=\mathrm{Ry}(\frac{2a_0-a_{0,new}}{a_0})=\mathrm{Ry}(\frac{2a_0-a_0(1+\delta)}{a_0})=\mathrm{Ry}(1-\delta)\qquad(\mathrm{eV}). \tag{17}$$

where the a_0 contraction /expansion factor δ was introduced. (17), using (7), provides

$$\mathrm{Ry}_{new}=\frac{a_{0V}F_{CV}}{e}(1-\delta)\qquad(\mathrm{eV}). \tag{18}$$

Then, when factor δ is negative, the atom contracts, so Ry_{new} is higher than Ry and the electron ought to increase its potential energy by this amount. When the atom restores to its initial radius, the electron would emit a photon having the input stress energy.

When the external stress is such that the atom radius increases, that is, $\delta > 0$, Ry_{new} is smaller than Ry. This time, the electron drops its potential energy by emitting a photon. When the stress is removed, the atom relaxes back to its normal radius and the electron recovers its original higher potential energy; obviously, no photon absorption takes place. Also, note that the above described processes occur only in non-ionized atoms and involve a single energy level. For electron transitions involving two stressed energy levels, it is necessary to reshape them using (18) in (8) and (12 to 14).

Example plots obtained using (18) are shown in Fig. 12 where δ is supposed to vary continuously and so do the output variables, namely, the energy level change, Fig. 12 *a*), and the emitted photon wavelength among any pair of quantum numbers; a few cases are given in Figs. 12 *b*) and *c*).

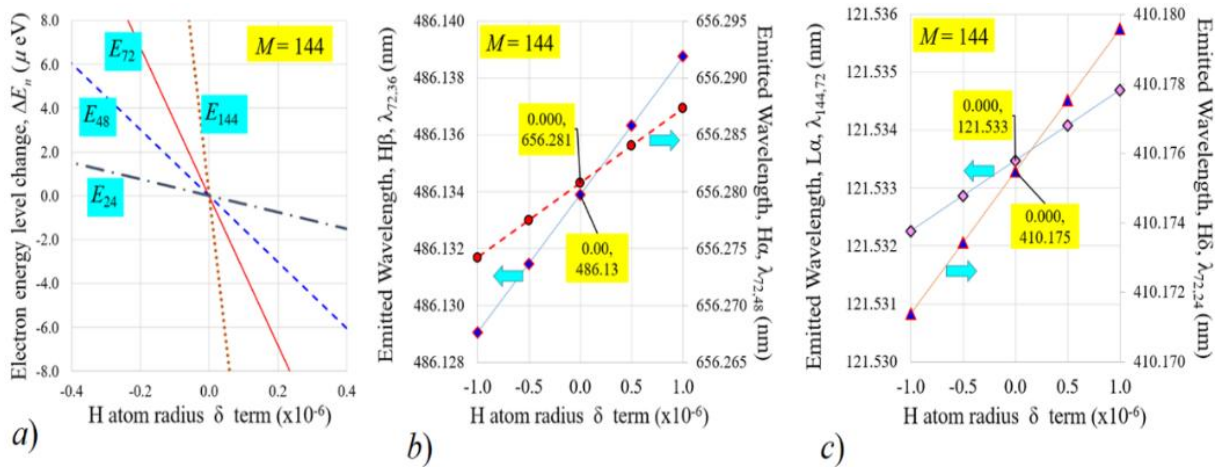

Figure 12 *a*) Electron allowed energy level change versus the H atom radius δ variation for the *M* = 144 transversal orbit model and *n* = 144, 72, 48, and 24. *b*) Effect of level energy change on the emitted wavelength for transitions among *n* = 72 to 36 (Hβ) and *n* = 72 to 48 (Hα). *c*) Shows the cases for *n* = 144 to 72 (Lyman-α) and for *n* = 72 to 24 (Hδ).

The needed a_0 δ values to produce the 21 and 28 cm radio astronomy lines for the transversal orbit model with $M = 48$ and $M = 144$ are given in Table H for n-energy values of M, M /2, M /4, M /24, M/48 and $n = 1$ for $M = 144$. For this emissions to happen, the electron thermal energy $1.5kT/e$ (eV), where k (J/°K) is Boltzmann constant and T (°K) is the absolute temperature, must be equal or higher than the energy level occupied by the electron, E_n, when the H atom radius is made to contract. The 21 and 28 cm photon energies relate to thermal energies changes corresponding to temperatures variations lower than 0.05 °K. That is why their experimental detection is not an easy task.

Table H. Use of (18) to derive the 21 and 28 cm H lines for M = 48 and M = 144 transversal orbit systems using selected energy n-levels given by M, $M/2$, $M/4$, $M/24$, $M/48$ and n = 1 for M = 144. For this model, the thermal activation energy is equal to the electron energy level.

	M = 48	M = 144		
a_0 δ term	n = 48 E (eV)	n = 144 E (eV)	E step (eV)	Emitted λ (cm)
0	13.602200000		//	//
-3.21420E-07	13.602204372		4.372E-06	28.3586
-4.31864E-07	13.602205874		5.874E-06	21.1062

	M = 48	M = 144		
a_0 δ term	n = 2 E (eV)	n = 6 E (eV)	E step (eV)	Emitted λ (cm)
0	0.023614931		//	//
-1.85140E-04	0.023619303		4.372E-06	28.3582
-2.48754E-04	0.023620805		5.874E-06	21.1062

	n = 24	n = 72		
a_0 δ term	E (eV)	E (eV)	E step (eV)	Emitted λ (cm)
0	3.400552500		//	//
-1.28568E-06	3.400556872		4.372E-06	28.3587
-1.72746E-06	3.400558374		5.874E-06	21.1062

	n = 1	n = 3		
a_0 δ term	E (eV)	E (eV)	E step (eV)	Emitted λ (cm)
0	0.005903733		//	//
-7.40560E-04	0.005908105		4.372E-06	28.3582
-9.95000E-04	0.005909607		5.874E-06	21.1065

	n = 12	n = 36		
a_0 δ term	E (eV)	E (eV)	E step (eV)	Emitted λ (cm)
0	1.511355556		//	//
-2.89300E-06	1.511359928		4.372E-06	28.3564
-3.88680E-06	1.511361430		5.874E-06	21.1061

	n = 1		
a_0 δ term	E (eV)	E step (eV)	Emitted λ (cm)
0.00000E+00	0.000655970	//	//
-6.66500E-03	0.000660342	4.372E-06	28.3584
-8.95520E-03	0.000661845	5.874E-06	21.1060

Equation (18) can also be applied to the electron energy levels given by the H Bohr model. The exact same results as above are obtained, see Table I. However, from the electron thermal energy point of view, conditions are quite different; the needed thermal excitation for the electron to reach a given n > 1 energy level, $\Delta E_{T,n}$ (eV), is much higher in Bohr model than for the transversal orbit model ; see values in Table I head line. For example, $\Delta E_{T,3}$ = 12.091 eV is associated to a thermal energy which implies a temperature of 93,540 °K.

Table I. Derivation of the 21 and 28 cm H lines for the H Bohr model for quantum numbers n = 1,2,3 and 24

a_0 δ term	n = 1 $\Delta E_{T,1}$ = 0.0 eV	E step (eV)	Emitted λ (cm)
0	13.602200000	//	//
-3.21420E-07	13.602204372	4.372E-06	28.359
-4.31864E-07	13.602205874	5.874E-06	21.106

a_0 δ term	n = 3 $\Delta E_{T,3}$ = 12.091 eV	E step (eV)	Emitted λ (cm)
0	1.511355556	//	//
-2.89300E-06	1.511359928	4.372E-06	28.356
-3.88680E-06	1.511361430	5.874E-06	21.106

a_0 δ term	n = 2 $\Delta E_{T,2}$ = 10.202 eV	E step (eV)	Emitted λ (cm)
0	3.400550000	//	//
-1.28568E-06	3.400554372	4.372E-06	28.359
-1.72746E-06	3.400555874	5.874E-06	21.106

a_0 δ term	n = 24 $\Delta E_{T,24}$ = 13.579 eV	E step (eV)	Emitted λ (cm)
0	0.023614931	//	//
-1.85140E-04	0.023619303	4.372E-06	28.358
-2.48754E-04	0.023620805	5.874E-06	21.106

Conclusions

It has been unveiled a H atom model based on a finite number of electron transversal orbits which can provide a good alternative to the Bohr model which is built upon an infinite quantum number implying an infinite radius orbit limit and an electron speed limit of zero. With a system of just $M = 48$ levels, the proposed model is able to predict the presence of the H emissions related to the well-known line series. Additionally, it delivers an excellent match to most lines appearing in Fraunhofer spectrum. Furthermore, the model predicts the presence of the emission lines which give rise to the so-called Fulcher bands within which numerous electron transition sequences would be produced. The 1128 calculated emission wavelengths of the 48 level model were presence-wise compared - showing a fairly good fit - against three segments of the NREL AM0 irradiance spectrum from the ultraviolet to the infrared ranges whose total data set amounts to 8813 spectral lines. Systems with $M = 144$ and $M = 216$ levels are shown to produce the level splitting or fine structure lines corresponding to the $D_{1,2,3}$ and $b_{1,2,3,4}$ bands in Fraunhofer spectrum; the same happens for the fine structures for the Lyman-α line and Balmer H- α line. The hyperfine structure galactic H lines with wavelengths of 21 and 28 cm can be detected for the transversal orbit model systems with $M = 2636$, partially, and up to $M = 7908$, fully. Finally, it was established that the hyperfine structure lines can be also produced in all allowed electron energy levels based on considering that the H atom is not rigid and its radius can be made to vary by external means. This holds true for both models considered here.

Notification

The authors declare that any potential conflict of interest exist regarding to the research, authorship and publication of this article.

Appendix. The H Bohr Model.

The Bohr fundamental assumption on the H atom electron angular momentum quantization affirms that

$$L_n = m_e v_n r_n = n\hbar \quad (\mathrm{J \cdot s}) \qquad n = 1, 2, 3, \ldots, \infty \tag{a}$$

where n is the quantum number, L_n (J·s) is n-orbit angular momentum, m_e (kg) is the electron rest mass, r_n (m) is the n-orbit radius, v_n (m/s) is the n-orbit electron velocity, $\hbar$ (J·s) is the Planck constant divided by 2π. The balance of the acting forces on the electron establishes that its centrifugal force, $E_{c,n}$ (N), equals its centripetal Columbian force, $F_{C,n}$ (N), and reads as

$$E_{c,n} = \frac{m_e v_n^2}{r_n} = \frac{e^2}{4\pi\varepsilon_0 r_n^2} = F_{C,n} \quad \text{(N)} \quad \text{for } n = 1, 2, 3, \ldots, \infty \tag{b}$$

where e (C) is the electron charge and ε_0 ($C^2/N/m^2$) is the vacuum permittivity. Solving (a) for v_n, inserting it in (b) and rearranging conduces to

$$r_n = \frac{\hbar}{m_e\{e^2/4\pi\varepsilon_0\hbar\}} n^2 = \frac{\hbar}{m_e v_1} n^2 = a_0 n^2 \quad \text{(m)} \quad \text{for } n = 1, 2, 3, \ldots, \infty \tag{c}$$

where v_1 (m/s) is the electron first orbit speed. (c), used back in (a), gives

$$v_n = \frac{n\hbar}{m_e a_0 n^2} = \frac{v_1}{n} \quad \text{(m/s)} \quad \text{for } n = 1, 2, 3, \ldots, \infty \tag{d}$$

Then, the allowed electron kinetic energy levels, E_n (eV), are given, after dividing by -e, by

$$-E_n = \frac{m_e v_n^2}{2e} = \frac{m_e v_1^2}{2en^2} = \frac{\text{Ry}}{en^2} \quad \text{(eV)} \quad \text{for } n = 1, 2, 3, \ldots, \infty \tag{e}$$

Table I gives an inventory of allowed electron energy levels E_n using (e) and the corresponding photon wavelength emitted when the electron transits into the n-energy level from the most separated initial energy level, or $n = \infty$, $\lambda_{\infty,n}$ and from its closest higher energy level $n = n + 1$, $\lambda_{n+1,n}$. For electron transitions into final energy levels with $n = 1$ to 6, these pairs of wavelengths represent the extreme values of the well-known H emission line series Lyman, Balmer, Paschen, Pfund and Humphreys, respectively. Only the Balmer series has a few lines in the visible range and are shown in italics.

The equations used for calculating the data presented in Table I are: 1) for the energy gap among an initial state i and a final state f is

$$E_{i,f} = \frac{Ry}{e}\frac{1-(f/i)^2}{f^2} \quad \text{(eV)} \quad \text{for } i = 2, 3, 4, \ldots, \infty; i > f = 1, 2, 3, 4, 5, 6 \tag{f}$$

and 2) for the corresponding electron transition, the emitted photon wavelength is obtained with

$$\lambda_{i,f} = \frac{hc}{E_{i,f}} 10^9 = \frac{1239.842}{E_{i,f}} \quad \text{(nm)} \quad \text{for } i = 2, 3, 4, \ldots, \infty; i > f = 1, 2, 3, 4, 5, 6 \tag{g}$$

Table I. Main Hydrogen line series in Bohr model. Selected inventory of the electron allowed *n*-energy levels and corresponding emitted photon wavelengths for $\lambda_{\infty,n}$ and $\lambda_{n+1,n}$ transitions.

n	$-E_n$(eV)	$\lambda_{\infty,n}$(nm)	$\lambda_{n+1,n}$(nm)	Lyman	Balmer	Paschen	Bracket	Pfund	Humphreys
1	**13.6022**	**91.15**	**121.53**	**121.5**					
2	3.4006	**364.6**	**656.3**	102.5	***656.28***				
3	1.5114	**820.4**	**1875.1**	97.2	*486.1*	**1875.1**			
4	0.8501	**1458.4**	**4051.1**	94.9	*434.0*	1281.8	**4051.1**		
5	0.5441	**2278.8**	**7457.7**	93.8	*410.2*	1093.8	2625.1	**7457.7**	
6	0.3778	**3281.4**	**12368.4**	93.0	*397.0*	1004.9	2165.5	4652.5	**12368.4**
7	0.2776	4466.4	19056.4	92.6	*388.9*	954.6	1944.5	3739.5	7500.4
8	0.2125	5833.6	27795.4	92.3	*383.5*	922.9	1817.4	3296.1	5906.5
9	0.1679	7383.2	38858.7	92.1	379.8	901.5	1736.2	3038.3	5127.2
10	0.1360	9115.0	22325.2	91.9	377.1	886.3	1680.6	2872.2	4671.2
11	0.1124	11029.2	13677.0	91.8	375.0	875.0	1640.7	2757.5	4375.2
12	0.0945	13125.6	13127.5	91.7	373.4	866.5	1610.9	2674.4	4169.6
24	0.0236	5.25E+04	6.70.E+05	91.30	366.95	832.3	1496.72	2373.70	3481.97
1000	1.36E-05	9.12E+07	4.56.E+10	91.15	364.60	820.4	1458.42	2278.81	3281.52
10000	1.36E-07	9.12E+09	4.56E+13	**91.15**	**364.60**	**820.35**	**1458.40**	**2278.75**	**3281.41**

References

[1] Niels Bohr, "On the constitution of atoms and molecules", Philos. Mag. 26 (6), 1-25, (July 1913) DOI: 10.1080/14786441308634955

[2] Kenneth W. Ford, "Teaching the Bohr atom," Letter to the Editor, Phys. Teach. **56**, 196 (April 2018). https://doi.org/10.1119/1.5028224

[3] Kenneth W. Ford, "Niels Bohr's First 1913 Paper: Still Relevant, Still Exciting, Still Puzzling" The Physics Teacher 56, 500 (October 2018); https://doi.org/10.1119/1.5064553

[4] The NIST Reference on Constants, Units, and Uncertainty, https://physics.nist.gov/cuu/Constants/ last accessed Dec/24/2022

[5] https://en.wikipedia.org/wiki/Fraunhofer_lines last accessed Dec/24/2022

[6] Adapted from https://en.wikipedia.org/wiki/Fraunhofer_lines#/media/File:Fraunhofer_lines.svg

[7] Gordon S. Fulcher, "Spectra of low potential discharges in air and hydrogen", The Astrophysical Journal 37: 60–71(1913) https://adsabs.harvard.edu/full/1913ApJ....37...60F

[8] Zhou Qing, D. K. Otorbaev, G. J. H. Brussaard, M. C. M. van de Sanden, D. C. Schram, "Diagnostics of the magnetized low-pressure hydrogen plasma jet: Molecular regime", Journal of Applied Physics 80, 1312 (1996); https://doi.org/10.1063/1.362930

[9] D. C. Schram, R. A. B. Zijlmans, O. Gabriel, R. Engeln, “Dissociative recombination as primary dissociation channel in plasma chemistry” Journal of Physics: Conference Series 192 (2009) 012012 https://doi.org/10.1088/1742-6596/192/1/012012

[10] Jeong-Jeung Dang, Kyoung-Jae Chunga, and Y. S. Hwang, “A simple spectroscopic method to determine the degree of dissociation in hydrogen plasmas with wide-range spectrometer” Review of Scientific Instruments 87, 053503 (2016); https://doi.org/10.1063/1.4948919

[11] S. V. Avtaeva, and T. M. LapochkinaD. “Characteristics of Molecular Hydrogen and CH* Radicals in a Methane Plasma in a Magnetically Enhanced Capacitive RF Discharge”, Plasma Physics Reports, 2007, Vol. 33, No. 9, pp. 774–785. © Pleiades Publishing, Ltd., 2007 https://doi.org/10.1134/S1063780X07090073

[12] NREL Air Mass Zero: Extraterrestrial Solar Irradiance Spectra https://www.nrel.gov/grid/solar-resource/spectra.html data file author Daryl Myers on 1/23/2004, downloaded Sept 2019.

[13] Fine structure https://en.wikipedia.org/wiki/Fine_structure last Dec/24/2022

[14] Randy Wayne, “Explanation of the fine structure of the spectral lines of hydrogen in terms of a velocity-dependent correction to Coulomb’s law”, The African Review of Physics (2015) 10:0043 https://www.semanticscholar.org/paper/EXPLANATION-OF-THE-FINE-STRUCTURE-OF-THE-SPECTRAL-A-Wayne/e84669921a878e5bc7459c8c855da498e8349a14#references

[15] H.C. van de Hulst, "Radio waves from space", Nederlandsch Tijdschrift voor Natuurkunde 11,201 -221 (1945) https://doi.org/10.1007/978-94-009-7752-5_34

[16] H.I. Ewen and E.M. Purcell, "Radiation from galactic hydrogen at 1420 Mc/s", Nature 168,356 - 357 (1951). https://ugrad.phys.unsw.edu.au/physoc/radio/21cmhyd.pdf

[17] C.A. Muller and J.H. Oort, "The interstellar hydrogen line at 1420 Mc/sec and an estimate of galactic rotation", Nature, Vol. 168, Issue 4270, pp. 357-358 (1951). https://doi.org/10.1038/168357a0